

Phase-Aware Single-Channel Speech Enhancement with Modulation-Domain Kalman Filtering

Nikolaos Dionelis, Student Member, IEEE, Mike Brookes, Member, IEEE

Abstract—We present a single-channel phase-sensitive speech enhancement algorithm that is based on modulation-domain Kalman filtering and on tracking the speech phase using circular statistics. With Kalman filtering, using that speech and noise are additive in the complex STFT domain, the algorithm tracks the speech log-spectrum, the noise log-spectrum and the speech phase. Joint amplitude and phase estimation of speech is performed. Given the noisy speech signal, conventional algorithms use the noisy phase for signal reconstruction approximating the speech phase with the noisy phase. In the proposed Kalman filtering algorithm, the speech phase posterior is used to create an enhanced speech phase spectrum for signal reconstruction. The Kalman filter prediction models the temporal/inter-frame correlation of the speech and noise log-spectra and of the speech phase, while the Kalman filter update models their nonlinear relations. With the proposed algorithm, speech is tracked and estimated both in the log-spectral and spectral phase domains. The algorithm is evaluated in terms of speech quality and different algorithm configurations, dependent on the signal model, are compared in different noise types. Experimental results show that the proposed algorithm outperforms traditional enhancement algorithms over a range of SNRs for various noise types.

Index Terms—Speech enhancement; single-channel; speech phase

I. INTRODUCTION

SPEECH enhancement in non-stationary noise environments is a challenging research area. The modulation domain is an often-used representation in models of the human auditory system; in speech enhancement, the modulation domain models the temporal/inter-frame correlation of frames rather than treating each frame independently [1] [2]. Enhancement algorithms can benefit from including a model of the inter-frame correlation of speech and a number of authors have found that the performance of a speech enhancer can be improved by using a speech model that imposes temporal structure [3], [4], [5]. Temporal inter-frame speech correlation modelling can be performed with a Kalman filter (KF) with a state of low dimension, as in [1] and [6]. The enhancement algorithms in [7] track the time evolution of the clean Short Time Fourier Transform (STFT) amplitude domain coefficients in every frequency bin. In [8], speech inter-frame correlation is modeled. Considering KF algorithms, many papers, such as [9] [10] and [11], utilise the nonlinear observation model relating clean and noisy speech in the log-spectral domain.

An overview of traditional statistical-based algorithms is given in [12]. Whereas traditional statistical-based algorithms treat each time-frame independently, an alternative approach

performs filtering in the modulation domain to model the time correlation of speech. Inter-frame speech correlation modelling can help enhancement algorithms achieve more noise reduction and less speech distortion [13]. Modulation-domain Kalman filtering refers to sequentially updating the statistics of speech utilising temporal constraints on the estimation of the speech spectrum with a KF prediction step [6], [7], [14]. In [15] and [16], KF tracking of speech (and noise in [17]) is presented. A number of authors perform speech Kalman filtering in the amplitude spectral domain assuming additivity of speech and noise in the same spectral domain [1], [18].

Existing enhancement KF algorithms that work in the time-frequency domain differ in their choice of the KF state, the KF prediction and the KF update. The KF state can be in the speech amplitude spectral domain [1] [18], the power spectral domain or the log-spectral domain [14] [19]. Speech spectra are well modelled by Gaussians in the log-spectral domain (and not so well in other domains), mean squared errors in the log-spectral domain are a good measure to use for perceptual speech quality and the non-negative log-spectral domain is most suitable for infinite-support Gaussian modelling.

Regarding the KF prediction, AR modelling with or without the AR mean can be performed based on the autocorrelation method, which uses windowing [20], or on the covariance method allowing or not allowing unstable AR poles. A KF with non-time-varying parameters requires the use of stable AR poles in the KF prediction, while a KF with time-varying parameters does not require the use of stable AR poles. Despite the observation that a time-varying KF does not require stable AR poles, the stability of the KF loop is still important.

The KF update is affected by the signal model that is used for the addition of speech and noise [21]. If speech and noise are independent, then they add in the complex STFT domain [22] [23]; it may however be analytically simpler to assume that speech and noise add either in the power spectral domain or the amplitude spectral domain [1] [18]. The aforementioned alternative possible ways are related to the phase factor, which is the cosine of the phase difference between speech and noise [22] [24]. Assuming speech and noise additivity in the power domain is equivalent to assuming that the phase factor is zero. Assuming speech and noise additivity in the amplitude domain is equivalent to assuming that the phase factor is equal to unity. The Kalman filtering algorithms in [1] and [18] assume that speech and noise are additive in the amplitude spectral domain, which results in noise oversubtraction in the region of 0 dB SNR that may sometimes be perceptually good [12].

Noise tracking using a KF can be beneficial for enhancement [25], [17]. Noise tracking is performed in [25] and subsequently in [26]. In the KF update step, the correlation

N. Dionelis and M. Brookes are with the Department of Electrical and Electronic Engineering, Imperial College London, London SW7 2AZ, U.K. (e-mail: nikolaos.dionelis11@imperial.ac.uk; mike.brookes@imperial.ac.uk).

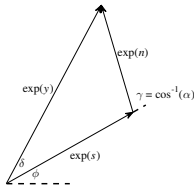


Figure 1. Plot of the STFT phasors in the complex plane.

between speech and noise can be estimated [14], [19].

Enhancement algorithms can benefit either from modelling the phase factor [14] or from estimating the speech phase [27]. The two related but distinct issues here are: (a) modelling the phase factor allows a better estimate of the speech amplitude, and (b) modelling the phase itself allows a better estimate of the speech phase. Both (a) and (b) can potentially improve the performance of the speech enhancer. Amongst other technical papers, the phase factor is considered in [22] and [28]. On the contrary, in [11], the phase factor is assumed to be zero. Estimating the speech phase and not estimating the noise phase does not affect the phase factor distribution; if the noise phase is uniformly distributed, then the difference of the speech phase and the noise phase is also uniformly distributed.

Recent research has shown the importance of estimating the speech phase [27] [29]: approximating the speech phase with the noisy phase can hinder the performance of enhancement algorithms. In recent years, the estimation of the speech phase is a widespread problem in speech processing [27]. The estimation of the speech phase as a circular quantity using circular probability distributions is a less widespread problem. Circular statistics take phase periodicity explicitly into account so that speech phase tracking does not fail when the discontinuity between $-\pi$ and π is reached [30].

In this paper, we perform phase-sensitive speech enhancement using a nonlinear modified KF in the log-spectral domain using speech phase tracking. Speech and noise are taken to be additive in the complex STFT domain, as in [14] [19]. Speech phase tracking can be beneficial for enhancement because successive segments of speech are correlated [31]. Modulation-domain Kalman filtering is performed using speech phase inter-frame correlation modelling and a phase-sensitive KF update that uses KF-based local priors for the speech phase. In the KF update, the posterior distributions of the speech phase and of the speech and noise log-spectra are computed using a specific four-dimensional distribution parametrisation.

The speech log-spectrum and phase and the noise log-spectrum are tracked using one KF for each frequency bin. A KF is utilised to deal with the temporal variability of speech: the temporal dynamics of the speech log-spectrum and phase are modelled using the KF prediction step. In the KF update, the estimated dynamics of the speech log-spectrum and phase are combined with the observed noisy log-spectrum and phase to obtain a minimum mean squared error (MMSE) estimate of the speech log-spectrum and phase. The ordinary technique in

order to incorporate the speech phase is to track and estimate either the complex STFT domain of speech or the real and imaginary parts of the STFT domain of speech [16] [32].

The structure of this paper is as follows. Section II presents the signal model, Sec. III describes the main phase-sensitive Kalman filtering algorithm that performs speech phase estimation and Sec. IV introduces the simplified versions of the main algorithm without speech phase estimation. The algorithms are evaluated in Sec. V and conclusions are drawn in Sec. VI.

II. SIGNAL MODEL AND NOTATION

In the time domain, the noisy speech signal, $\tilde{y}(l)$, is given by $\tilde{y}(l) = \tilde{s}(l) + \tilde{n}(l)$, where $\tilde{s}(l)$ and $\tilde{n}(l)$ are the clean speech and additive noise respectively and l is the discrete time index. Applying the STFT, we obtain $Y_t(k) = S_t(k) + N_t(k)$ where t indexes the time-frame and k the frequency bin. Within the KF algorithm, frequency bins are processed independently and, for clarity in the remainder of this paper, the frequency index, k , is omitted and the time-frame index, t , is included only in equations that involve multiple time-frames.

In the complex STFT domain, we have: $Y = S + N \Leftrightarrow |Y|e^{j\theta} = |S|e^{j\phi} + |N|e^{j\psi}$ where the noisy speech phase is θ , the speech phase is ϕ and the noise phase is ψ . The STFT spectral log-amplitudes of the noisy speech, speech and noise are denoted by $y = \log |Y|$, $s = \log |S|$ and $n = \log |N|$.

Taking the complex logarithm of the STFT coefficients gives $e^{y+j\theta} = e^{s+j\phi} + e^{n+j\psi}$. We define the relative phases of the noisy speech and noise by $\delta = \theta - \phi$ and $\gamma = \psi - \phi$ respectively. Figure 1 depicts the STFT phasors in the complex plane including the angles δ and γ . Substituting for θ and ψ gives $e^{y+j\delta} = e^s + e^{n+j\gamma}$. We note that if δ, γ lie in the range $[-\pi, \pi)$ then, since e^s is real and positive, δ and γ have the same sign, $\text{sgn}(\delta) = \text{sgn}(\gamma)$; this will be used in Sec. III.D.

For convenience, we also define the phase factor, $\alpha = \cos \gamma$. If S and N are independent, then γ is uniform, $\gamma \sim U(-\pi, \pi)$, and the phase factor distribution, $p(\alpha)$, is given by

$$p(\alpha) = \begin{cases} \frac{1}{\pi \sqrt{1-\alpha^2}} & \text{if } -1 < \alpha < 1 \\ 0 & \text{otherwise.} \end{cases} \quad (1)$$

Equation (1) is also utilised in [14], [19] and [28].

In this paper, the semicolon “;” is used to denote vertical concatenation of vectors: $(\mathbf{x}_1; \mathbf{x}_2) = (\mathbf{x}_1^T \mathbf{x}_2^T)^T$. In addition, \mathcal{Y}_t is used to denote all the noisy complex STFT coefficients up to time t . Furthermore, the notation $s_{t|t} = \mathbb{E}\{s_t | \mathcal{Y}_t\}$ is utilised to denote the posterior of a random variable, s_t .

A. Circular distributions and moments

The distribution of a phase, ϕ , is commonly modelled using either the von Mises (vM) distribution or the Wrapped Normal (WN) distribution which are both defined by two parameters. In both cases, the distribution can be uniquely defined by its complex-valued first circular moment, $E(\exp(j\phi))$ [30]. The vM distribution and its first circular moment are given by

$$p_{\text{vM}}(\phi; \mu^{(\phi)}, \kappa^{(\phi)}) = \frac{\exp(\kappa^{(\phi)} \cos(\phi - \mu^{(\phi)}))}{2\pi I_0(\kappa^{(\phi)})} \quad (2)$$

and

$$\mathbb{E}\{\exp(j\phi)\} = \exp(j\mu^{(\phi)}) \frac{I_1(\kappa^{(\phi)})}{I_0(\kappa^{(\phi)})} \quad (3)$$

respectively. In (2) and (3), $I_0(x)$ is the Bessel function of the order zero and, in (3), $I_1(x)$ is the Bessel function of the order one [30]. In addition, in (2) and (3), $\mu^{(\phi)}$ is the mean and $\kappa^{(\phi)}$ is the concentration of the vM distribution. We denote the vM distribution with mean $\mu_t^{(\phi)}$ and concentration $\kappa_t^{(\phi)}$ by $\text{vM}(\mu_t^{(\phi)}, \kappa_t^{(\phi)})$. For a given complex-valued first trigonometric moment, $m_1 = |m_1|e^{j\angle m_1}$, the vM distribution with this first moment has the density $\text{vM}(\angle m_1, \frac{I_0(|m_1|)}{I_1(|m_1|)})$ [30].

The WN distribution and its first circular moment are

$$p_{\text{WN}}(\phi; \mu^{(\phi)}, \sigma^{2(\phi)}) = \frac{1}{\sigma^{(\phi)}\sqrt{2\pi}} \sum_{k=-\infty}^{\infty} \exp\left(\frac{-(\phi - \mu^{(\phi)} + 2\pi k)^2}{2\sigma^{2(\phi)}}\right) \quad (4)$$

and

$$\mathbb{E}\{\exp(j\phi)\} = \exp(j\mu_t^{(\phi)} - 0.5\sigma_t^{2(\phi)}) \quad (5)$$

respectively. In (4) and (5), $\mu_t^{(\phi)}$ is the mean and $\sigma_t^{2(\phi)}$ is the variance of the WN distribution. We denote the WN distribution with mean $\mu_t^{(\phi)}$ and variance $\sigma_t^{2(\phi)}$ by $\text{WN}(\mu_t^{(\phi)}, \sigma_t^{2(\phi)})$. For a given complex-valued first trigonometric moment, $m_1 = |m_1|e^{j\angle m_1}$, the WN distribution with this first moment has the probability density $\text{WN}(\angle m_1, -2\log(|m_1|))$ [30].

III. DESCRIPTION OF THE ENHANCEMENT ALGORITHM

A. Overview of the Algorithm

The algorithm's flowchart is shown in Fig. 2. The core of the algorithm is the KF enclosed in the figure by a dashed line. The KF tracks the posterior distributions of the speech phase and of the log-spectra of both the speech and the noise. Rather than tracking the speech phase, ϕ , directly, it is more convenient to track the unit-magnitude complex quantity, $\exp(j\phi)$.

The first step of the algorithm is to transform the noisy speech signal into the time-frequency domain using the STFT. The algorithm considers the spectral amplitude and phase of the noisy speech separately. The noisy spectral amplitude is used in three ways: (a) it is converted to the log-power domain and used as the KF observation together with the noisy phase, θ , (b) it is pre-cleaned and used for speech AR modelling of order p in the log-spectral domain, and (c) it is used for noise AR modelling of order q in the log-spectral domain. The noisy phase is converted to the complex domain and then used for speech phase complex AR modelling of order 1.

For the prediction step of the KF, autoregressive AR models are estimated for $\exp(j\phi)$ and for the log-spectra of speech and noise. To estimate the speech log-spectrum AR model, the noisy speech spectrum is pre-cleaned using a conventional speech enhancer, converted to the log-power domain and then divided into overlapping modulation frames followed by AR analysis. To estimate the AR model for $\exp(j\phi)$, the noisy

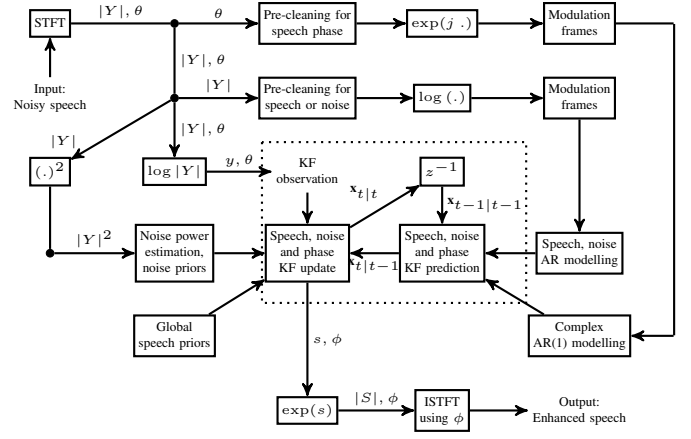


Figure 2. The flowchart of the algorithm is illustrated. The blocks in the dotted rectangle constitute the KF that tracks the speech and noise log-spectra, (s, n) , and the speech phase, ϕ . The term z^{-1} refers to one-frame delay.

phase is pre-cleaned using a speech phase enhancer, converted to the complex domain and then divided into overlapping modulation frames followed by AR analysis.

The linear KF prediction step (described in Sec III.B) uses the results of the AR analysis to predict the KF state in the current frame, t , from previous observations.

The KF update (described in Sec. III.D) is nonlinear and combines the output of the KF prediction with the observed noisy speech log-spectrum and phase while incorporating additional prior distributions for the speech and noise log-spectra. The additional prior distribution of the noise is determined using an independent noise estimator. The global speech prior distribution is obtained by multiplying an offline-trained speech model by the estimated active speech level [33].

The final step of the algorithm is to extract the estimated phase and log-power of the current frame from the KF state vector and to combine these to generate the corresponding STFT coefficient. The inverse STFT (ISTFT) is then used to reconstruct the enhanced speech signal in the time domain.

B. The KF state and the KF prediction step

In Fig. 2, within the dotted rectangle, the KF state vector, \mathbf{x}_t , has dimension $(p + q + 1)$ and may be partitioned as

$$\mathbf{x}_t = \begin{pmatrix} \mathbf{x}_t^{(s)}; \mathbf{x}_t^{(n)}; x_t^{(p)} \end{pmatrix} \quad (6)$$

where

$$\mathbf{x}_t^{(s)} = (s_t \ s_{t-1} \ \dots \ s_{t-p+1})^T \in \mathfrak{R}^p \quad (7)$$

$$\mathbf{x}_t^{(n)} = (n_t \ n_{t-1} \ \dots \ n_{t-q+1})^T \in \mathfrak{R}^q \quad (8)$$

$$x_t^{(p)} = \exp(j\phi_t) \in \mathbb{C}. \quad (9)$$

Based on equations (6)-(9), the speech KF state is $\mathbf{x}_t^{(s)}$, the noise KF state is $\mathbf{x}_t^{(n)}$ and the phase KF state is $x_t^{(p)}$. For the speech KF state, $\mathbf{x}_t^{(s)}$, the speech signal model is

$$\mathbf{x}_{t|t-1}^{(s)} = \mathbf{A}_t^{(s)} \begin{pmatrix} \mathbf{x}_{t-1|t-1}^{(s)} - \zeta_t^{(s)} \end{pmatrix} + \zeta_t^{(s)} + \mathbf{w}_t^{(s)} \quad (10)$$

where

$$\mathbf{A}_t^{(s)} = \begin{pmatrix} -\mathbf{a}_t^{(s)T} \\ \mathbf{I} \ \mathbf{0} \end{pmatrix} \in \mathfrak{R}^{p \times p} \quad (11)$$

$$\mathbf{Q}_t^{(s)} = \begin{pmatrix} \epsilon_t^{(s)} & \mathbf{0}^T \\ \mathbf{0} & \mathbf{0} \end{pmatrix} \in \mathfrak{R}^{p \times p}. \quad (12)$$

Equation (10) is the linear KF prediction equation that is based on AR modelling and on (11) and (12).

In (10)-(12), the speech KF transition matrix is $\mathbf{A}_t^{(s)}$, the speech KF transition noise covariance matrix is $\mathbf{Q}_t^{(s)}$ and the speech KF transition noise is $\mathbf{w}_t^{(s)}$. The speech KF transition noise, $\mathbf{w}_t^{(s)}$, is zero-mean Gaussian with covariance matrix $\mathbf{Q}_t^{(s)}$. In addition, the vector of speech AR coefficients is $\mathbf{a}_t^{(s)} \in \mathfrak{R}^p$ and the variance of the transition noise is $\epsilon_t^{(s)}$. The prior of the speech KF state is denoted by $\mathbf{x}_{t|t-1}^{(s)}$ and the posterior of the speech KF state at time $(t-1)$ is denoted by $\mathbf{x}_{t-1|t-1}^{(s)}$.

In (10), $\mathbf{A}_t^{(s)}$, $\zeta_t^{(s)}$ and $\mathbf{Q}_t^{(s)}$ are estimated from AR(p) modelling described in Sec III.G. The AR mean, $\zeta_t^{(s)}$, is the mean speech log-amplitude estimated as a speech AR parameter.

In (10), the way in which the speech KF state, $\mathbf{x}_t^{(s)}$, changes in the speech KF prediction step is defined. The speech KF state consists of a speech KF state mean, $\boldsymbol{\mu}_t^{(s)} \in \mathfrak{R}^p$, and a speech KF state covariance matrix, $\mathbf{P}_t^{(s)} \in \mathfrak{R}^{p \times p}$. Both $\boldsymbol{\mu}_t^{(s)}$ and $\mathbf{P}_t^{(s)}$ are updated in the linear speech KF prediction using

$$\boldsymbol{\mu}_{t|t-1}^{(s)} = \mathbf{A}_t^{(s)} \left(\boldsymbol{\mu}_{t-1|t-1}^{(s)} - \zeta_t^{(s)} \right) + \zeta_t^{(s)} \quad (13)$$

$$\mathbf{P}_{t|t-1}^{(s)} = \mathbf{A}_t^{(s)} \mathbf{P}_{t-1|t-1}^{(s)} \mathbf{A}_t^{(s)T} + \mathbf{Q}_t^{(s)}. \quad (14)$$

For the noise KF state, $\mathbf{x}_t^{(n)}$, the inter-frame correlation between adjacent noise frames is modelled in the log-spectral domain using a noise KF prediction step that is based on noise AR(q) modelling described in Sec III.G. As in (13) and (14), the noise KF prediction step equations are

$$\boldsymbol{\mu}_{t|t-1}^{(n)} = \mathbf{A}_t^{(n)} \left(\boldsymbol{\mu}_{t-1|t-1}^{(n)} - \zeta_t^{(n)} \right) + \zeta_t^{(n)} \quad (15)$$

$$\mathbf{P}_{t|t-1}^{(n)} = \mathbf{A}_t^{(n)} \mathbf{P}_{t-1|t-1}^{(n)} \mathbf{A}_t^{(n)T} + \mathbf{Q}_t^{(n)} \quad (16)$$

where the quantities with the superscript (n) refer to the noise KF state and are analogous to the speech quantities.

The algorithm uses a joint speech and noise KF state with a full covariance matrix, hence tracking the correlation between speech and noise in the log-spectral domain [14]. The joint speech and noise KF state is $\mathbf{x}_t^{(j)} = (\mathbf{x}_t^{(s)}; \mathbf{x}_t^{(n)}) \in \mathfrak{R}^{p+q}$. The superscript (j) denotes the joint KF state. For the joint KF state, $\mathbf{x}_t^{(j)}$, the joint speech and noise signal model is

$$\mathbf{x}_{t|t-1}^{(j)} = \mathbf{A}_t^{(j)} \left(\mathbf{x}_{t-1|t-1}^{(j)} - \zeta_t^{(j)} \right) + \mathbf{w}_t^{(j)} + \zeta_t^{(j)} \quad (17)$$

where

$$\mathbf{A}_t^{(j)} = \begin{pmatrix} \mathbf{A}_t^{(s)} & \mathbf{0} \\ \mathbf{0} & \mathbf{A}_t^{(n)} \end{pmatrix} \in \mathfrak{R}^{(p+q) \times (p+q)} \quad (18)$$

$$\zeta_t^{(j)} = (\zeta_t^{(s)}; \dots; \zeta_t^{(s)}; \zeta_t^{(n)}; \dots; \zeta_t^{(n)}) \in \mathfrak{R}^{(p+q)} \quad (19)$$

$$\mathbf{Q}_t^{(j)} = \begin{pmatrix} \mathbf{Q}_t^{(s)} & \mathbf{0} \\ \mathbf{0} & \mathbf{Q}_t^{(n)} \end{pmatrix} \in \mathfrak{R}^{(p+q) \times (p+q)}. \quad (20)$$

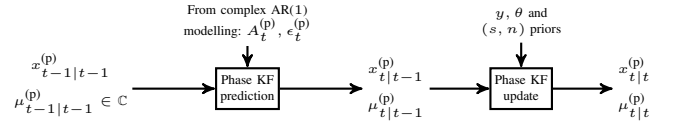


Figure 3. The speech phase KF is shown. The inputs and outputs in this diagram match the inputs and outputs of the dotted rectangle in Fig. 2 only for the speech phase KF. The speech phase KF state is $x_t^{(p)} = \exp(j\phi_t)$.

The KF prediction step update equations for the mean, $\boldsymbol{\mu}_t^{(j)}$, and covariance matrix, $\mathbf{P}_t^{(j)}$, are therefore

$$\boldsymbol{\mu}_{t|t-1}^{(j)} = \mathbf{A}_t^{(j)} \left(\boldsymbol{\mu}_{t-1|t-1}^{(j)} - \zeta_t^{(j)} \right) + \zeta_t^{(j)} \quad (21)$$

$$\mathbf{P}_{t|t-1}^{(j)} = \mathbf{A}_t^{(j)} \mathbf{P}_{t-1|t-1}^{(j)} \mathbf{A}_t^{(j)T} + \mathbf{Q}_t^{(j)} \quad (22)$$

$$\boldsymbol{\mu}_{t|t}^{(j)} = \left(\boldsymbol{\mu}_{t|t}^{(s)}; \boldsymbol{\mu}_{t|t}^{(n)} \right) \in \mathfrak{R}^{(p+q)} \quad (23)$$

$$\mathbf{P}_{t|t}^{(j)} = \begin{pmatrix} \mathbf{P}_{t|t}^{(s)} & \mathbf{Z}^T \\ \mathbf{Z} & \mathbf{P}_{t|t}^{(n)} \end{pmatrix} \in \mathfrak{R}^{(p+q) \times (p+q)} \quad (24)$$

where $\mathbf{P}_t^{(j)}$ can be decomposed as shown in the last line.

For the speech phase KF state, $x_t^{(p)}$, $\exp(j\phi_t)$ is utilised. Using $\exp(j\phi_t)$ as the speech phase KF state leads to $E\{\exp(j\phi_t)\exp(-j\phi_t)\} = 1$ and, in turn, this leads to (25). The speech phase KF state variance, $P_t^{(p)} \in \mathfrak{R}$, is related to the speech phase KF state mean, $\mu_t^{(p)} \in \mathbb{C}$, with

$$P_t^{(p)} = 1 - |\mu_t^{(p)}|^2. \quad (25)$$

Due to (25), the algorithm tracks the phase KF state mean, $\mu_t^{(p)}$, and does not utilise $P_t^{(p)}$. In (6), the KF state, $\mathbf{x}_t \in \mathbb{C}^{p+q+1}$, is defined and, now, the KF state mean is

$$\boldsymbol{\mu}_{t|t-1} = \left(\boldsymbol{\mu}_{t|t-1}^{(j)}; \mu_{t|t-1}^{(p)} \right). \quad (26)$$

It should be noted that $\boldsymbol{\mu}_t$ and $\mathbf{P}_t^{(j)}$ do not correspond to each other. According to (26), $\boldsymbol{\mu}_t$ includes both $\boldsymbol{\mu}_{t|t-1}^{(j)}$ and $\mu_{t|t-1}^{(p)}$.

Figure 3 shows how the speech phase KF state, $x_t^{(p)}$, evolves over time. The three main points of Fig. 3 are: (a) only $\mu_t^{(p)}$ is used to track $x_t^{(p)}$, (b) $x_{t|t-1}^{(p)}$ is computed from $x_{t-1|t-1}^{(p)}$ and from the two parameters of complex AR(1) modelling, and (c) the speech phase posterior, $x_{t|t}^{(p)}$, given the noisy y and θ is calculated using the correlated log-spectrum local priors of (s, n) . Regarding (b), the two parameters of the complex AR(1) modelling are the AR coefficient, $A_t^{(p)} \in \mathbb{C}$, and the speech phase KF transition noise variance, $\epsilon_t^{(p)} \in \mathfrak{R}$.

Equations (27)-(30) show how $\mu_t^{(p)}$ changes in the speech phase KF prediction step. To perform the KF prediction step, $\check{\mu}_{t|t-1}^{(p)}$ is first obtained from the AR model. Moment matching is then used to map this to a WN distribution with parameters $\check{\mu}_{t|t-1}^{(\phi)}$ and $\check{\sigma}_{t|t-1}^{2(\phi)}$. Next, the transition noise variance, $\epsilon_t^{(p)}$, is added onto $\check{\sigma}_{t|t-1}^{2(\phi)}$ and is then converted back to the first circular moment, $\mu_{t|t-1}^{(p)}$. These steps are summarised as:

$$\check{\mu}_{t|t-1}^{(p)} = A_t^{(p)} \mu_{t-1|t-1}^{(p)} \quad (27)$$

$$\check{\mu}_{t|t-1}^{(\phi)} = \text{atan2} \left(\Im \{ \check{\mu}_{t|t-1}^{(p)} \}, \Re \{ \check{\mu}_{t|t-1}^{(p)} \} \right) \quad (28)$$

$$\check{\sigma}_{t|t-1}^{2(\phi)} = -2 \log(|\check{\mu}_{t|t-1}^{(p)}|) \quad (29)$$

$$\mu_{t|t-1}^{(p)} = \exp \left(j \check{\mu}_{t|t-1}^{(\phi)} - 0.5 \left(\check{\sigma}_{t|t-1}^{2(\phi)} + \epsilon_t^{(p)} \right) \right). \quad (30)$$

Considering the uncertainty in the complex AR prediction, the transition noise variance, $\epsilon_t^{(p)}$, reduces the absolute value of $\mu_t^{(p)}$. Equations (27)-(30) are based on the WN distribution and on trigonometric moment matching in Sec. II.A.

Full covariance matrices are not used to model the correlation between the speech phase, ϕ , and the speech and noise log-spectra, (s, n) . The algorithm assumes $p(s, n, \phi) = p(s, n) p(\phi)$ and thus that ϕ is independent of (s, n) .

C. The nonlinear KF update step

The algorithm performs the update $\mathbf{x}_{t|t} = (\mathbf{x}_{t|t}^{(j)}; x_{t|t}^{(p)})$. The Kalman filtering algorithm first estimates $x_{t|t}^{(p)}$ using

$$\mu_{t|t}^{(p)} = \mathbb{E} \left\{ x_{t|t}^{(p)} \mid \mathcal{Y}_t \right\} \quad (31)$$

and it then computes $\mathbf{x}_{t|t}^{(j)}$.

To perform the KF update, the KF state vector, $\mathbf{x}_{t|t-1}$, is first transformed so that the elements corresponding to the current time, $(s_t; n_t)$, are uncorrelated with the other elements [7]. The current-frame elements, $(s_t; n_t)$, are decorrelated in the KF state because the proposed KF update is nonlinear. Then, the mean and the covariance matrix of these elements are updated as described in Sec III.D. Finally, the transformation is reversed in order to restore the original KF state vector.

In the KF prediction presented in Sec. III.B, the priors, $\mu_{t|t-1}^{(j)}$ and $\mathbf{P}_{t|t-1}^{(j)}$, are calculated in (23) and (24). In the KF update in Sec. III.D, the posteriors, $\check{\mu}_{t|t}^{(j)}$ and $\check{\mathbf{P}}_{t|t}^{(j)}$, are found. This section shows how the decorrelation and recorelation steps are used to calculate $\mu_{t|t}^{(j)}$ and $\mathbf{P}_{t|t}^{(j)}$.

Before performing the KF update, the KF state is decorrelated by multiplying the speech and noise state vector, $\mathbf{x}^{(j)}$, by the matrix \mathbf{D} . The transformation matrix, \mathbf{D} , is chosen to decorrelate the current frame elements, s_t and n_t , from the rest of the state vector. Transformed quantities are identified with a breve diacritic. The multiple-element decorrelation operation preserves the inter-frame correlation that is created from the KF prediction step so that the algorithm performs the KF update with the variables in the current time-frame.

The covariance matrix, $\mathbf{P}_{t|t-1}$, is first decomposed as

$$\mathbf{P}_{t|t-1}^{(j)} = \begin{pmatrix} \mathbf{P}_A & \mathbf{P}_B^T \\ \mathbf{P}_B & \mathbf{P}_C \end{pmatrix}. \quad (32)$$

Then, $\mathbf{D} = \mathbf{C}\mathbf{B}$ is utilised where

$$\mathbf{C} = \begin{pmatrix} \mathbf{I} & \mathbf{0} \\ -\mathbf{P}_B \mathbf{P}_A^{-T} & \mathbf{I} \end{pmatrix} \quad (33)$$

and where the permutation matrix $\mathbf{B} \in \mathfrak{R}^{(p+q) \times (p+q)}$ is

$$\mathbf{B} = [e_1 \ e_{p+1} \ e_2 \ e_3 \ \dots \ e_p \ e_{p+2} \ e_{p+3} \ \dots \ e_{p+q}]^T \quad (34)$$

where e_i is the i -th column of the identity matrix. Next, \mathbf{D} is used along with the linear transformation

$$\check{\mu}_{t|t-1}^{(j)} = \mathbf{D} \mu_{t|t-1}^{(j)} \quad (35)$$

$$\check{\mathbf{P}}_{t|t-1}^{(j)} = \mathbf{D} \mathbf{P}_{t|t-1}^{(j)} \mathbf{D}^T \triangleq \begin{pmatrix} \mathbf{P}_A & \mathbf{0} \\ \mathbf{0} & \mathbf{P}_C - \mathbf{P}_B \mathbf{P}_A^{-1} \mathbf{P}_B^T \end{pmatrix} \quad (36)$$

where the off-diagonal block matrices are zero matrices. The decorrelation step is the linear transformation in (35), (36).

For convenience, from (36), we also define

$$\check{\check{\mathbf{P}}}_C = \mathbf{P}_C - \mathbf{P}_B \mathbf{P}_A^{-1} \mathbf{P}_B^T. \quad (37)$$

In (32) and (36), we observe that \mathbf{P}_A is preserved after the multiple-element decorrelation operation. This is important since \mathbf{P}_A is updated in the KF update in Sec. III. D. After the KF update, the inverse transformation is applied with

$$\mu_{t|t}^{(j)} = \mathbf{D}^{-1} \check{\mu}_{t|t}^{(j)} \quad (38)$$

$$\mathbf{P}_{t|t}^{(j)} = \mathbf{D}^{-1} \check{\mathbf{P}}_{t|t}^{(j)} (\mathbf{D}^T)^{-1}. \quad (39)$$

Equations (38) and (39) constitute the recorelation step.

In (38) and (39), the posteriors $\check{\mu}_{t|t}^{(j)}$ and $\check{\mathbf{P}}_{t|t}^{(j)}$ are computed using the equations in (40) and (41). Now, $\check{\mu}_{t|t}^{(j)}$ is defined by:

$$\check{\mu}_{t|t}^{(j)} = \left(s_{t|t}; n_{t|t}; \check{\mu}_{C,t|t-1}^{(j)} \right), \quad \check{\mu}_{C,t|t-1}^{(j)} \in \mathfrak{R}^{(p+q-2)} \quad (40)$$

$$\text{where } \check{\mu}_{t|t-1}^{(j)} = \left(s_{t|t-1}; n_{t|t-1}; \check{\mu}_{C,t|t-1}^{(j)} \right)$$

where the $s_{t|t}$ notation is introduced in Sec. II. Furthermore, the posterior covariance matrix, $\check{\mathbf{P}}_{t|t}^{(j)}$, is defined by:

$$\check{\mathbf{P}}_{t|t}^{(j)} = \begin{pmatrix} \check{\mathbf{P}}_{A,t|t} & \mathbf{0} \\ \mathbf{0} & \check{\mathbf{P}}_{C,t|t-1} \end{pmatrix} \quad (41)$$

$$\text{where } \check{\mathbf{P}}_{t|t-1}^{(j)} = \begin{pmatrix} \check{\mathbf{P}}_{A,t|t-1} & \mathbf{0} \\ \mathbf{0} & \check{\mathbf{P}}_{C,t|t-1} \end{pmatrix}$$

$$\check{\mathbf{P}}_{A,t|t} \in \mathfrak{R}^{2 \times 2}, \quad \check{\mathbf{P}}_{C,t|t-1} \in \mathfrak{R}^{(p+q-2) \times (p+q-2)}$$

$$\check{\mathbf{P}}_{A,t|t} = \begin{pmatrix} \mathbb{E} \{ s_t^2 \mid \mathcal{Y}_t \} & \mathbb{E} \{ s_t n_t \mid \mathcal{Y}_t \} \\ \mathbb{E} \{ s_t n_t \mid \mathcal{Y}_t \} & \mathbb{E} \{ n_t^2 \mid \mathcal{Y}_t \} \end{pmatrix} - \begin{pmatrix} s_{t|t} & n_{t|t} \end{pmatrix} \begin{pmatrix} s_{t|t} & n_{t|t} \end{pmatrix}^T.$$

In Sec III.D, $\mathbb{E} \{ (s_t; n_t; x_t^{(p)}) \mid \mathcal{Y}_t \}$ is calculated along with the covariance matrix of the first two elements of this vector.

D. The phase-sensitive modified KF update

This section describes the evaluation of the quantities needed to perform the KF update step described in Sec II.C, namely the posterior distribution parameters $(s_{t|t}; n_{t|t}; \mu_{t|t}^{(p)})$ in (40) and (31) together with the speech and noise covariance matrix $\check{\mathbf{P}}_{t|t}^{(j)}$ in (41). The algorithm tracks the complex-valued

speech phase posterior mean, $\mu_{t|t}^{(p)}$, without its real-valued variance due to $\boldsymbol{\mu}_{t|t} = (\boldsymbol{\mu}_t^{(i)}; \mu_t^{(p)})$ in (26).

In this section, the time subscript, t , is omitted from all the random variables for clarity, as described in Sec. II.

The prior distribution, $p(s, n, \phi, \psi) = p(s, n) p(\phi) p(\psi)$, may be obtained from the KF prediction step outputs, $\boldsymbol{\mu}_{t|t-1}$ and $\mathbf{P}_{t|t-1}^{(i)}$, together with the assumption that ψ is uniformly distributed, $\psi \sim U(-\pi, \pi)$. To impose the observation constraint, we use the relationship $e^{y+j\delta} = e^s + e^{n+j\gamma}$ illustrated by the STFT phasor diagram in Fig. 1. We assume that $p(s, n, \phi, \psi)$ can be decomposed as the product of three independent distributions over the domain $-\infty < s, n < \infty$ and $-\pi < \phi, \psi \leq \pi$. To calculate the conditional distribution for a given observation, y_t and θ_t , we make a change of variables and we parametrise the distribution using (u, y, γ, θ) . This invertible and one-to-one transformation is given by:

$$u = n - s \quad (42)$$

$$y = 0.5(s + n + \log(2 \cosh(u) + 2 \cos \gamma)) \quad (43)$$

$$\theta = \phi + \delta \quad (44)$$

$$= \phi + \operatorname{sgn}(\gamma) \cos^{-1} \left(\frac{e^{2y} + e^{2s} - e^{2n}}{2e^{s+y}} \right)$$

$$= \phi + \operatorname{sgn}(\gamma) \cos^{-1} (\cosh(y - s) - 0.5e^{2n-s-y}).$$

Equations (42)-(44) are over the domain $-\infty < u, y < \infty$ and $-\pi < \gamma, \theta \leq \pi$, assuming $0 \leq \cos^{-1}(\cdot) \leq \pi$.

Equation (43) is the nonlinear log-spectral distortion equation, which is also in [11]. Equation (43) can be derived by multiplying $e^{y+j\delta} = e^s + e^{n+j\gamma}$ by its complex conjugate and taking logs. Multiplying $e^{y+j\delta} = e^s + e^{n+j\gamma}$ by its complex conjugate gives $e^{2y} = e^{s+n} (e^{s-n} + e^{n-s} + 2 \cos \gamma)$.

In addition, equation (44) can be derived by writing $e^{y+j\theta} - e^{s+j\phi} = e^{n+j\psi}$ and multiplying this equation by its complex conjugate, which gives $e^{2y} + e^{2s} - 2e^{s+y} \cos \delta = e^{2n}$.

The inverse transformation of (42)-(44) is given by:

$$v = s + n = 2y - \log(2 \cosh(u) + 2 \cos \gamma) \quad (45)$$

$$s = 0.5(v - u), \quad n = 0.5(v + u) \quad (46)$$

$$\delta = \operatorname{sgn}(\gamma) \quad (47)$$

$$\times \cos^{-1} (\cosh(y - s) - 0.5e^{2n-s-y})$$

$$\phi = \theta - \delta, \quad \psi = \gamma + \phi. \quad (48)$$

We use $(s, n, \phi, \psi) \Rightarrow (u, y, \gamma, \theta)$. The Jacobian matrix, $\frac{\partial(u, y, \gamma, \theta)}{\partial(s, n, \phi, \psi)}$, is computed and the Jacobian is $\Delta = 1$.

Now, we form the conditional distribution $p(u, \gamma | y, \theta)$ to apply the observation constraint. To calculate the posterior mean and covariance matrices, $\check{\boldsymbol{\mu}}_{t|t}^{(i)}$ and $\check{\mathbf{P}}_{t|t}^{(i)}$, that are required in (38) and (39), we compute expectations of the form:

$$\mathbb{E}\{f(\cdot) | y_t, \theta_t\} = \int_{u, \gamma} f(\cdot) p(u, \gamma | y_t, \theta_t) du d\gamma$$

$$\propto \int_{u, \gamma} f(\cdot) p(u, \gamma, y_t, \theta_t) du d\gamma \quad (49)$$

$$= \int_{u, \gamma} f(\cdot) |\Delta|^{-1} p(s, n, \phi, \psi) du d\gamma$$

$$\propto \int_{u, \gamma} f(\cdot) p(s, n, \phi, \psi) du d\gamma$$

$$= \int_{u, \gamma} f(\cdot) p(s, n) p(\phi) p(\psi) du d\gamma$$

where (s, n, ϕ, ψ) are obtained from $(u, \gamma, y_t, \theta_t)$ using the equations in (45)-(48). In (49), the speech phase, ϕ , is assumed to be independent of the speech and noise log-powers.

Based on Sec. II, $\psi \sim U(-\pi, \pi)$ and thus (49) becomes:

$$\mathbb{E}\{f(\cdot) | y_t, \theta_t\} \propto \int_{u, \gamma} f(\cdot) p(s, n) p(\phi) du d\gamma. \quad (50)$$

In (49)-(50), we compute conditional expectations and we use $f(\cdot)$ to denote any function $f(u, y, \gamma, \theta)$. We can now calculate a conditional expectation and we can then split the integral into two regions according to the sign of γ :

$$\mathbb{E}\{f(\cdot) | y_t, \theta_t\} \propto \int_{u, \gamma} f(\cdot) p(s, n) p(\phi) du d\gamma \quad (51)$$

$$= \int_{-\pi}^0 \int_u f(\cdot) p(s, n) p(\phi | \gamma \leq 0) du d\gamma$$

$$+ \int_0^{\pi} \int_u f(\cdot) p(s, n) p(\phi | \gamma > 0) du d\gamma.$$

We now make the one-to-one transformation $\alpha = \cos \gamma$ separately for each of the two integrals in (51):

$$\mathbb{E}\{f(\cdot) | y_t, \theta_t\} \quad (52)$$

$$= \int_{\alpha} \int_u f(\cdot) p(s, n) p(\phi | \gamma \leq 0) |\Delta_{\alpha}|^{-1} du d\alpha$$

$$+ \int_{\alpha} \int_u f(\cdot) p(s, n) p(\phi | \gamma > 0) |\Delta_{\alpha}|^{-1} du d\alpha$$

where both integrals are over the domain $-\infty < u < \infty$ and $-1 < \alpha < 1$. In (52), $\Delta_{\alpha} = \frac{d\alpha}{d\gamma} = -\sqrt{1 - \alpha^2}$.

Using (52), the first and second moments of $(s, n, x_t^{(p)})$ are computed. Due to $p(s, n, \phi) = p(s, n) \times p(\phi)$, the correlations between s and ϕ and between n and ϕ are always zero in the KF prior distribution but are not zero in the KF posterior.

Using $0 \leq a + b \leq 2$, where a and b are non-negative integers, we now compute the posterior for (s, n) . We utilise $p(\alpha)$ as defined in (1). The posterior for (s, n) is based on:

$$\mathbb{E}\{s^a n^b | y_t, \theta_t\} \propto \int_{\alpha} \frac{1}{\sqrt{1 - \alpha^2}}$$

$$\times \int_u s^a n^b \times p(u, v) p(\phi | \gamma \leq 0) du d\alpha \quad (53)$$

$$+ \int_{\alpha} \frac{1}{\sqrt{1 - \alpha^2}} \times \int_u s^a n^b \times p(u, v) p(\phi | \gamma > 0) du d\alpha$$

where v is defined in (45) based on y, u and $\alpha = \cos \gamma$. In (53), $p(\phi)$ is utilised along with the mapping from $E\{x_t^{(p)}\}$ to $p(\phi)$ using the vM distribution presented in Sec. II.A.

Moreover, using equation (52), in order to compute the posterior for $x_t^{(p)}$, we now compute:

$$\begin{aligned} \mathbb{E} \left\{ x_t^{(p)} \mid y_t, \theta_t \right\} &\propto \int_{\alpha} \frac{1}{\sqrt{1-\alpha^2}} \\ &\int_u \exp(j\phi \mid \gamma \leq 0) p(u, v) p(\phi \mid \gamma \leq 0) du d\alpha + \\ &\int_{\alpha} \frac{1}{\sqrt{1-\alpha^2}} \int_u \exp(j\phi \mid \gamma > 0) p(u, v) p(\phi \mid \gamma > 0) du d\alpha. \end{aligned} \quad (54)$$

Equations (53) and (54) provide the link between Sec. III.C and Sec. III.D. With (54), we compute $\mu_{t|t}^{(p)}$ in (31) and with (53), we calculate $(s_{t|t}; n_{t|t})$ in (40). Finally, with (53), we find $\mathbb{E} \{s_t^2 \mid \mathcal{Y}_t\}$, $\mathbb{E} \{s_t n_t \mid \mathcal{Y}_t\}$ and $\mathbb{E} \{n_t^2 \mid y_t, \mathcal{Y}_t\}$ in (41).

E. Summary and discussion of the KF update

The proposed KF update uses that speech and noise are additive in the complex STFT domain. The KF update computes the posterior of the speech and noise log-spectra and of the speech phase. The phase-aware KF update is presented in (42)-(54) and uses a local prior for the speech phase from the phase KF prediction in Fig. 3. Using such a speech phase local prior, which is based on inter-frame speech phase modelling, is different from using the pitch and intra-frame phase correlation modelling [27] [31]. The KF update computes the speech phase posterior using the speech phase local prior together with the speech and noise log-spectra local priors.

With (54), the complex-valued first trigonometric moment for the speech phase posterior is estimated. As mentioned in Sec. II.A, the vM and WN distributions can be computed from the complex-valued first trigonometric moment with moment matching [30]. For the phase posterior, the speech phase concentration, $\kappa_{t|t}^{(\phi)}$, of the vM distribution can be calculated. There is a strong correlation between $\kappa_{t|t}^{(\phi)}$ and the estimated speech log-spectrum. For voiced frames, $\kappa_{t|t}^{(\phi)}$ is large, which means that the posterior variance is small, and the estimated clean speech log-spectrum, $s_{t|t}$, is high. Conversely, in silence or unvoiced frames, $\kappa_{t|t}^{(\phi)}$ is small and $s_{t|t}$ is relatively low.

Figure 4 illustrates the KF prior and posterior distributions when the KF update presented in (42)-(54) is utilised. Figure 4 depicts the speech and noise KF posterior and omits the phase KF posterior. The background in Fig. 4 is based on the covariance matrix of the KF posterior and the ellipses are the covariance matrices of the KF prior and posterior distributions. In Fig. 4, we use $y = 0$, $\theta = 0$ and $\mu^{(\phi)} = 0.66$ and $\kappa^{(\phi)} = 3.01$ for the vM distribution of the speech phase, ϕ .

In Fig. 4, the speech and noise KF posterior lies within the curvy triangle, which is mathematically defined by:

$$\alpha = 1, \quad \cosh(u) = 0.5 \exp(-v) \quad (55)$$

$$\alpha = -1, \quad |\sinh(u)| = 0.5 \exp(-v). \quad (56)$$

The curvy triangle defines the KF observation constraint region in the (s, n) plane. The curvy triangle in Fig. 4 and in (55), (56) is related to the different values that the phase factor can take [14]. In Fig. 4, the KF prior is in the curvy triangle and on the $u = 0$ line, which is for a SNR of 0 dB.

Figure 5 resembles Fig. 4 but, now, the KF prior is in the curvy triangle and off the $u = 0$ line. Figures 4, 5 are important

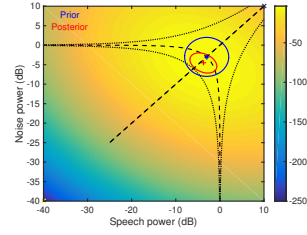


Figure 4. Plot of the KF posterior, the KF prior, the $\alpha = -1, 0, 1$ constraint lines and the $u = 0$ line.

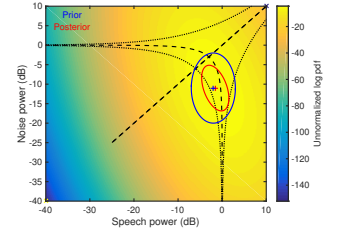


Figure 5. Plot of the KF posterior, the KF prior, the $\alpha = -1, 0, 1$ constraint lines and the $u = 0$ line.

because they show that the KF posterior should lie within the curvy triangle and the KF observation constraint region.

Finally, equations (42)-(54) describe the proposed nonlinear modified KF update that is different from the normal linear KF update and is based on the decorrelation and correlation steps in Sec. III.C. The KF algorithm uses probability distributions and statistical inference instead of an observation equation.

To sum up, in Secs. III.B-D, a Kalman filtering algorithm that performs ϕ tracking using both inter-frame ϕ modelling (with the speech phase KF prediction) and ϕ estimation (with the nonlinear KF update) is designed. The KF is a powerful estimator and its potential is exploited as far as possible by using speech phase, ϕ , tracking. In Sec. III.D, the KF update based on the decorrelation and recorrelation steps introduced in Sec. III.C is formulated. Finally, as in [24], iterated KF updates, and thus two iterations of the proposed nonlinear KF update step presented in (42)-(54), can be performed.

F. The non-KF-based priors in the KF loop

In this section, we present how we use the uncorrelated priors for speech and noise that are not based on the KF prediction. The non-KF-based uncorrelated priors for speech and noise are the global speech priors and the noise priors.

The KF-based local prior is

$$p(s_t, n_t, \phi_t \mid \mathcal{Y}_{t-1}) = p(s_t, n_t \mid \mathcal{Y}_{t-1}) p(\phi_t \mid \mathcal{Y}_{t-1}). \quad (57)$$

In (57), we assume that the speech phase, ϕ , is independent of (s, n) , as in (49).

In (57), we note that $p(\phi_t \mid \mathcal{Y}_{t-1})$ is the KF-based local speech phase prior, the output of the phase KF prediction in Sec. III.B after using the notation introduced in Sec. II.A and trigonometric moment matching to the vM distribution.

The next step is to consider the global speech prior and the noise prior. Up to this point, we have not included the global speech prior and the noise prior in our model. If we utilise the global speech prior and the noise prior, then (57) becomes:

$$\begin{aligned} p(s_t, n_t, \phi_t \mid \mathcal{Y}_{t-1}, \mathcal{G}^{(s)}, \mathcal{G}^{(n)}) \\ = p(s_t, n_t \mid \mathcal{Y}_{t-1}, \mathcal{G}^{(s)}, \mathcal{G}^{(n)}) p(\phi_t \mid \mathcal{Y}_{t-1}) \end{aligned} \quad (58)$$

where $\mathcal{G}^{(s)}$ is the global knowledge from the global speech prior and $\mathcal{G}^{(n)}$ is the knowledge from the noise prior.

In (58), for $p(s_t, n_t \mid \mathcal{Y}_{t-1}, \mathcal{G}^{(s)}, \mathcal{G}^{(n)})$, we now have:

$$p(s_t, n_t | \mathcal{Y}_{t-1}, \mathcal{G}^{(s)}, \mathcal{G}^{(n)}) \propto p(s_t, n_t | \mathcal{Y}_{t-1}) p(s_t | \mathcal{G}^{(s)}) p(n_t | \mathcal{G}^{(n)}). \quad (59)$$

In (59), $p(s_t, n_t | \mathcal{Y}_{t-1}, \mathcal{G}^{(s)}, \mathcal{G}^{(n)})$ is the result of the multiplication of the correlated KF-based local prior for speech and noise, $p(s_t, n_t | \mathcal{Y}_{t-1})$, by the global speech prior and by the noise prior. Both the global speech prior and the noise prior are assumed to be Gaussian distributions. When the local prior has a small variance, the algorithm chooses this estimate because of the Gaussian-Gaussian multiplication in (59).

G. The processing outside the KF loop

We now describe the processing that is carried outside the KF loop (i.e. the dotted rectangle) in Fig. 2. The “pre-cleaning for speech” in the “pre-cleaning for speech or noise” block in Fig. 2 applies a conventional enhancement algorithm (e.g. the Log-MMSE estimator [34]) to the noisy speech, as in [1] [2] and in [35]. The speech is then divided into overlapping modulation frames in the log-spectral domain and AR(p) modelling is performed to estimate the coefficients $\mathbf{a}_t^{(s)}$, $\zeta_t^{(s)}$ and $\epsilon_t^{(s)}$ from (10). AR modelling is performed using the covariance method, estimating the AR coefficients and the AR mean. Estimating the speech AR mean, $\zeta_t^{(s)}$, as an AR coefficient is beneficial because we operate in the log-spectral domain and so $\zeta_t^{(s)}$ represents a scale factor in the amplitude domain. The AR coefficients need to be estimated from noisy speech and their estimate is inevitably biased. When speech pre-cleaning is used, the model misspecification error is reduced [1].

The “pre-cleaning for noise” in the “pre-cleaning for speech or noise” block in Fig. 2 uses a voice activity detection (VAD) that is based on an AR(1) one-pole smoother, as in [7], and on the estimated SNR from the KF state. The VAD computes $\hat{n}_t = \lambda_t \hat{n}_{t-1} + (1 - \lambda_t) y_t$, where \hat{n} denotes the noise estimate and λ_t is obtained from applying a sigmoid function to the estimated SNR, $\eta_t = \exp(2s_t - 2n_t)$. The estimation of the noise parameters $\mathbf{a}_t^{(n)}$, $\zeta_t^{(n)}$ and $\epsilon_t^{(n)}$ from (15), (16) are created from noise AR(q) modelling in the same way as for speech.

The “pre-cleaning for speech phase” block in Fig. 2 performs speech phase pre-cleaning using the speech phase estimator in [31] prior to the estimate of the speech phase AR model in order to reduce AR modelling errors.

In summary, in Sec. III, we presented the KF algorithm in Fig. 2. We discussed how to track the speech and noise log-spectra in combination with the speech phase, ϕ . We also utilised (s, n, ϕ, ψ) from which we can define all the other variables presented in Sec. II including the noisy y and θ .

IV. DESCRIPTION OF THE SIMPLIFIED ALGORITHMS

In this section, the various ways in which the algorithm in Sec. III can be simplified are presented. Simplified algorithms help to identify which blocks are the most significant.

A. Tracking only the speech log-spectrum

We now track speech in the log-spectral domain using one KF for each frequency bin. Without KF noise tracking, before the KF update step, the (s, n) priors are uncorrelated.

We use the speech KF state, $\mathbf{x}_t \in \mathbb{R}^p$, and the speech KF prediction in (10)-(14). Then, we use the one-element decorrelation operation, which is a specific case of the multiple-element decorrelation operation in (35) and (36), before the KF update. The KF update estimates the posterior distribution of the speech and noise log-spectra. Based on Sec. II:

$$e^{2y} = e^{2s} + e^{2n} + 2e^{s+n}\alpha. \quad (60)$$

From (60): $\alpha = 0.5 \exp(2y - s - n) - \cosh(u)$, where $u = n - s$. It should be noted that u was utilised in Sec. III.D and in (42). We also use $y = 0.5(s + n + \log(2(\alpha + \cosh(u))))$.

The variable transformation $(s, n, \alpha) \Rightarrow (u, y, \alpha)$ is then performed. The Jacobian determinant is $\Delta_2 = 1$. Now, the posterior distribution given the noisy log-amplitude, y , is:

$$p(u, \alpha | y) = \frac{p(u, \alpha, y)}{p(y)} \Big|_y \propto \left(p(s, n) p(\alpha) |\Delta_2|^{-1} \right) \Big|_y \quad (61) \\ \propto p(\alpha) \mathcal{N} \left(\begin{pmatrix} 2y - \log(2(\alpha + \cosh(u))) - u \\ 2y - \log(2(\alpha + \cosh(u))) + u \end{pmatrix}; \mathbf{m}, \mathbf{S} \right)$$

where a Gaussian distribution with mean \mathbf{m} and covariance matrix \mathbf{S} is used for $p(s, n)$, as in [14]. We find the moments of the posterior distribution using

$$\mathbb{E}\{s^a n^b | y\} = \int_{\alpha=-1}^1 \int_{u=-\infty}^{\infty} s^a n^b p(u, \alpha | y) du d\alpha \\ = \frac{1}{|\Delta_2| p(y)} \int_{\alpha=-1}^1 p(\alpha) \int_{u=-\infty}^{\infty} s^a n^b p(s, n) du d\alpha \quad (62)$$

where $0 \leq a + b \leq 2$, $s = s(u, y, \alpha)$ and $n = n(u, y, \alpha)$.

We update the mean and covariance matrix of the current speech-noise KF state. We calculate the first and second moments of the posterior distribution of the current speech and noise log-spectra, (s, n) , using $E\{s^a n^b | y\}$ in (60), (61).

B. Alternative KF updates

The KF updates in Sec. III.D and Sec. IV.A use that speech and noise are additive in the complex STFT domain. Four alternative ways to do the KF update are now considered. The first way is to assume speech and noise additivity in the power spectral domain and that speech and noise follow a Gaussian distribution in the log-spectral domain. We denote this method by AP that refers to additivity in the power spectral domain. Assuming additivity in the power spectral domain, which is equivalent to assuming $\alpha = 0$ and that speech and noise are in-quadrature, is an intermediate case of the proposed KF updates in Sec. III.D and Sec. IV.A that use $\alpha \in [-1, 1]$.

The second alternative way is to assume speech and noise additivity in the amplitude domain and that speech and noise are Gaussian in the log-spectral domain. We denote this technique by AA that refers to additivity in the amplitude spectral domain. Assuming speech and noise additivity in the amplitude domain, which is equivalent to assuming $\alpha = 1$ and that speech and noise are in-phase, is an extreme case of the proposed KF updates in Sec. III.D and Sec. IV.A.

The third alternative way is to assume speech and noise additivity in the power spectral domain and that the speech and

noise are Gaussian in the power domain. To do this, we convert the log-power domain speech and noise distributions into the power domain by matching the first and second moments. We denote this method by APPG that refers to additivity in the power spectral domain with power-domain Gaussians.

The fourth alternative way is to assume speech and noise additivity in the amplitude domain and that the speech and noise are Gaussian in the amplitude domain. To do this, we convert the log-domain speech and noise distributions into the amplitude domain by matching the first and second moments. We denote this technique by AAAG that refers to additivity in the amplitude domain with amplitude-domain Gaussians.

C. Tracking only the speech and noise log-spectra

We now describe a simplified version of the KF algorithm of Fig. 2 that tracks the speech and noise log-spectra. Based on III.B, with noise tracking, the KF state $\in \mathbb{R}^{p+q}$ is the speech KF state $\in \mathbb{R}^p$ and the noise KF state $\in \mathbb{R}^q$. Moreover, with noise tracking, the (s, n) local priors are correlated: we track the correlation between the speech and noise log-spectra.

We use the joint speech-noise KF state, $\mathbf{x}_t^{(j)}$, and the speech and noise KF prediction described in Sec. III.B and in (10)-(16). We then use the multiple-element decorrelation operation in (35) and (36), before the KF update. Next, we perform the KF update that is presented in Sec. IV.A and in (61)-(62).

We now define the algorithm acronyms for the proposed Kalman filtering algorithms. We denote the algorithm presented in Sec. IV.A by ST that refers to speech tracking (ST). Correspondingly, we denote the KF algorithm presented in Sec. IV.C by SNT that refers to ST and noise tracking (NT). In addition, we also denote the Kalman filtering algorithm that performs speech phase estimation presented in Sec. III by SNPT that refers to SNT and phase tracking (PT).

V. IMPLEMENTATION

For the implementation of the Kalman filtering algorithm, we use acoustic frames of length 32 ms, an acoustic frame time increment of 8 ms, modulation frames of 64 ms and a modulation frame time increment of 8 ms. We use a full overlap for the modulation frames. We use speech utterances from the TIMIT database [36] sampled at 16 kHz. We use noise recordings from the RSG-10 database [37] at SNR levels from -20 dB to 30 dB. Randomly selected noise segments are used in each test and noisy speech is created using [38].

For the noise prior, we use external noise estimation based on [39]. For speech amplitude spectrum pre-cleaning, we use the Log-MMSE estimator [34]. The KF state dimensions for speech and noise are respectively $p = 2$ and $q = 2$. In addition, for speech phase pre-cleaning in Fig. 2, we utilise [31].

A. Evaluation of Integrals

We now present the integration details of the KF update of the proposed algorithm in Sec. III.D and in Sec. IV.A. In (52)-(54) and in (62), we integrate over the phase factor and over u . The outer integration over the phase factor, α , is done with R sigma points [14]. The inner integration over u is performed

either by numerical integration or by approximating the range in segments with truncated Gaussian distributions.

We utilise $\mathbb{E}\{\alpha^c\}$, and $\mathbb{E}\{\alpha^c\} = 2^{-c}c!((0.5c)!)^{-2}$ for even c and zero otherwise, for the outer integration over α in (52)-(54) and in (62). The outer integration over α is done using the Unscented transform [40] and weighted sigma points for approximating integration with summation [21]. We fit the first six moments of the phase factor, α , using (1) and

$$\mathbb{E}\{\alpha^c\} = \int_{\alpha=-\infty}^{\infty} p(\alpha) \alpha^c d\alpha = \sum_{r=1}^R w_r \alpha_r^c. \quad (63)$$

The outer integral over α in (52)-(54) and in (62) is exact to $f(\alpha)$ polynomials up to the fifth order in (63), when $R = 3$. For $R = 3$, $w_r = 0.333 \forall r$ and $\alpha_r = \{0, \pm\sqrt{0.75}\}$. Using $R = 3$ sigma points produces better results than using $R = 1$ and using $R = 5$ produces similar results to using $R = 3$.

For the integration over u , we use numerical integration. An alternative way is to utilise straight line segments with truncated Gaussian distributions in order to obtain a closed-form approximation. Based on Sec. III.E and on Figs. 4-5 that show the (s, n) plane, for v in terms of u , it is possible to approximate the range in segments with truncated Gaussian distributions. In (52)-(54) and in (62), a small number of straight line segments in which v is linearly approximated in u for a given α can be used. In (52)-(54), ϕ is a complicated function of u and a small number of straight line segments in which ϕ is linearly approximated in u for a given α can also be utilised. The function of ϕ in terms of u is in (45)-(48).

B. Computational complexity

In this section, we provide a brief analysis on the computational requirements of the different configurations of the proposed modulation-domain Kalman filtering algorithm. The estimation formulas in Secs. III-IV describe the computation for each frame of noisy speech and for each frequency bin.

As in [41], we compute the average real-time factor so as to evaluate the computational efficiency (i.e. the latency) of the presented algorithm. For the simplified KF algorithm in Sec. IV.A with an acoustic frame length of 32 ms, an acoustic time increment of 16 ms, a modulation frame of 128 ms and a modulation time increment of 64 ms, the average real-time factor is 28 using a laptop equipped with an Intel Core i5 processor. Using the same machine, the average real-time factor of the algorithm in [41] is 4; the algorithm in [41] is 7 times faster than the proposed algorithm leading to the conclusion that one of the main disadvantages of the proposed Kalman filtering algorithm is its computational efficiency.

For the algorithm in Sec. III, the real-time factor is between 30 and 50 using the same machine, dependent on the acoustic and modulation frame parameters. In Sec. III, we reconstruct the speech phase for all frequencies and not up to 4 kHz, as in [31], because the nonlinear KF update in Sec. III. D is a joint speech log-amplitude and phase estimator and, in high frequencies, estimating the speech amplitude is important.

We observe a tradeoff between accuracy and computational complexity. For high accuracy, we want a small acoustic frame time increment [29] and a short modulation frame length.

For a perceptual comparison, the reader is referred to [42] where some recordings processed by the KF are available.

VI. EVALUATION

The KF algorithm is compared with certain state-of-the-art approaches to speech enhancement. We compare the different algorithm configurations in Secs. III-IV with: (a) the traditional technique of Log-MMSE [34] with the MMSE noise estimator [39], and (b) the optimally modified log-spectral amplitude (OMLSA) estimator [43] with the improved minima controlled recursive averaging (IMCRA) noise estimator [44].

We compare the ST algorithm with the alternative KF updates that are introduced and discussed in Sec. IV.B. The alternative KF updates in Sec. IV.B constitute the KF baselines of this paper and the algorithms (a)-(b), in the previous paragraph, constitute the non-KF baselines of this paper.

Table I summarizes the nine different algorithms that are considered in this section. ST, SNT and AP were also evaluated in [14] and ST and SNT were also evaluated in [19]. Based on Sec. IV.B, Table I presents the different combinations of the signal model and the KF state. The horizontal bold labels correspond to the KF state domains that define the domain in which the KF prediction is performed. In addition, the vertical bold labels correspond to the signal model domains that define the domain in which additivity between speech and noise is assumed and/or used in the KF update step.

Table I

The 9 different algorithms that are considered and the different combinations of the domains of the signal model and the KF state. The rows and columns refer to the signal model domains and the KF state domains respectively.

	Log-spectral	Amplitude	Power
STFT	ST	-	-
Amplitude	AA	AAAG	-
Power	AP	-	APPG
SNT	SNPT	Log-MMSE	OMLSA

The structure of the evaluation section is as follows. Section VI.A presents the evaluation metrics and Sec. VI.B compares the Kalman filtering algorithm with the baselines Log-MMSE and OMLSA. Section VI.C examines the signal model and KF state domains and Sec. VI.D examines the quantities that are tracked. Based on Secs. I-IV and on Table I, Kalman filtering depends on the signal model domain, on the KF state domain and on the quantities that are tracked. Finally, Sec. VI.E considers the quality metrics presented in Sec. VI.A.

A. Quality metrics

The algorithms are evaluated in terms of speech quality with the Perceptual Evaluation of Speech Quality (PESQ) metric [45] and with the speech quality (SIG), the noise quality (BAK) and the overall speech quality (OVRL) metrics [46].

B. Comparison with the non-KF baseline algorithms

In this section, we evaluate the different configurations of the proposed modulation-domain Kalman filtering algorithm.

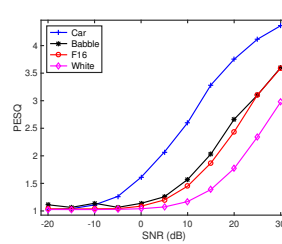


Figure 6. Plot of the mean PESQ scores for noisy speech versus SNR for the noise types used in evaluation.

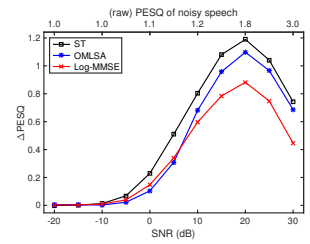


Figure 7. Plot of the mean Δ PESQ for speech with white noise versus SNR for the speech-only KF (ST) and two conventional algorithms.

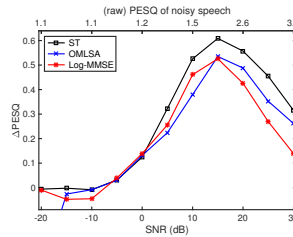


Figure 8. Plot of the mean Δ PESQ for speech with additive babble noise.

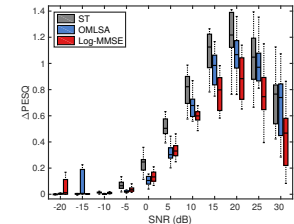


Figure 9. Boxplot of the Δ PESQ for speech with additive white noise.

We use the core test set of the TIMIT database in order to evaluate the presented algorithm and its different configurations in different noise types. The number of sentences in the TIMIT core test is 192; the TIMIT core test contains 16 male and 8 female speakers each reading 8 distinct sentences. The algorithms are examined across different speaking rates.

Figure 6 shows the different types of noise that are used in Sec. VI for evaluation purposes and presents the (raw) PESQ scores for the noisy speech signals. Figure 6 depicts the raw PESQ scores for car, babble, F16 aircraft and white noises. As seen in Fig. 6, the noise types of babble and F16 have small differences in their effects at a particular SNR.

The main enhancement algorithm of this paper is SNPT, which is presented in Sec. III. We evaluate SNPT and we also evaluate the simpler algorithms of ST and SNT, which are presented in Sec. IV, so as to assess the relative contribution of each of the blocks of the main algorithm. In this way, the contribution of ST and SNT to the final PESQ improvement, Δ PESQ, of SNPT will be assessed. The ST algorithm is first evaluated and compared with the two non-KF baselines, Log-MMSE and OMLSA, using Δ PESQ. Then, the more complex versions of the Kalman filtering algorithm, SNT and SNPT, will be compared with ST using Δ PESQ.

Figure 7 illustrates the mean of the Δ PESQ scores of ST, OMLSA and Log-MMSE for white noise in various SNRs. The ST algorithm is better than the other algorithms for $-10 < \text{SNR} \leq 30$ dB. In Fig. 7, the top horizontal axis shows the (raw) PESQ of noisy speech for white noise; the top horizontal axis in Fig. 7 matches the white noise curve in Fig. 6. Figure 6 shows that white noise decreases PESQ more than the other noise types of car, babble and F16. Moreover, Fig. 7 shows that the enhancement algorithms increase PESQ a lot because white noise is a stationary non-speech-shaped noise type.

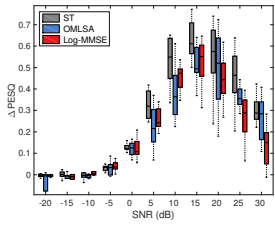
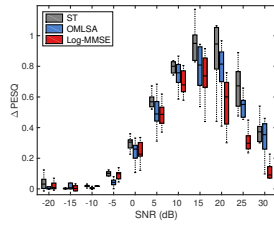
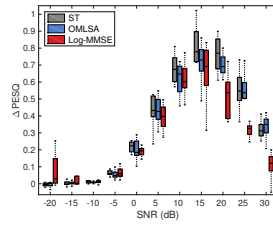
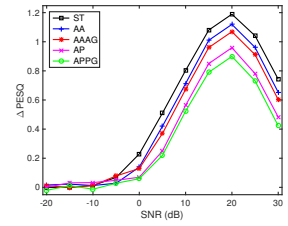
Figure 10. Boxplot of the Δ PESQ for speech with additive babble noise.Figure 11. Boxplot of the Δ PESQ scores for speech with F16 noise.Figure 12. Boxplot of the Δ PESQ for speech with additive car noise.Figure 13. Plot of the mean Δ PESQ for speech with additive white noise versus SNR showing the effect of using different signal models.

Figure 8 depicts the mean Δ PESQ scores of ST, OMLSA and Log-MMSE for babble noise. We observe that the Δ PESQ scores are lower in Fig. 8 than in Fig. 7 since babble noise is non-stationary. Figure 8 shows that ST is better than the two non-KF baseline algorithms for $0 < \text{SNR} \leq 30$ dB. In Fig. 8, the top horizontal axis shows the (raw) PESQ of noisy speech for babble noise; in other words, the top horizontal axis in Fig. 8 matches the black babble noise curve in Fig. 6.

Figure 9 illustrates the median and the interquartile range of the Δ PESQ scores of ST, OMLSA and Log-MMSE for white noise. Based on both Figs. 7 and 9, the ST algorithm is better than the two baseline algorithms for $-10 < \text{SNR} \leq 30$ dB.

The legends of all the figures, and of all the boxplots like Fig. 9, have the same order as the curves in high SNRs.

Figure 10 shows the median and the interquartile range of the Δ PESQ scores of ST, OMLSA and Log-MMSE for babble noise. Likewise, Fig. 11 illustrates the median and the interquartile range of the Δ PESQ scores of ST, OMLSA and Log-MMSE for F16 noise. Figure 10 shows that ST is better than the two non-KF baselines for $5 < \text{SNR} \leq 30$ dB for babble noise. In addition, Fig. 11 shows that ST is better than the two baselines for $0 < \text{SNR} \leq 30$ dB for F16 noise.

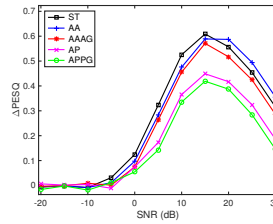
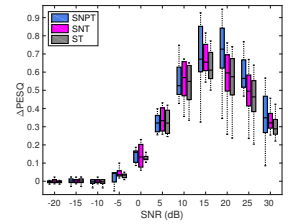
Figures 9-11 are boxplots and examine the variability and the inter-quartile range of the Δ PESQ scores. We observe that the three algorithms do not have comparable Δ PESQ variability. Boxplots also illustrate the frequent best and worst enhancement cases; for clarity, the infrequent best and worst enhancement cases (i.e. the outliers) are not included. Based on Fig. 9, at 20 dB SNR white noise, ST can have a Δ PESQ of 1.41 in the frequent case and a Δ PESQ of 0.79 in the frequent worst case. Also, based on Fig. 10, at 15 dB SNR babble, ST can have a Δ PESQ of 0.74 in the frequent best case and a Δ PESQ of 0.49 in the frequent worst case.

Figure 12 is a boxplot of the Δ PESQ scores of ST, Log-MMSE and OMLSA for car noise. Figure 12 shows that ST is better than and/or comparable to the Log-MMSE and OMLSA baselines for the SNR range of $-10 < \text{SNR} \leq 30$ dB.

C. Choice of signal model

We now compare ST, which is presented in Sec. IV.A, with the alternative KF updates presented in Sec. IV.B that use a simpler signal model and assume $\alpha = 0$ or $\alpha = 1$. Both the ST algorithm and the main enhancement algorithm SNPT, which is presented in Sec. III, use the phase factor distribution.

We compare Kalman filtering algorithms that use different signal models. In Figs. 13,14, we compare ST with AP, AA,

Figure 14. Plot of the mean Δ PESQ for speech with additive babble noise.Figure 15. Boxplot of the Δ PESQ for speech with babble noise versus SNR showing the effect of tracking different quantities in the KF.

APPG and AAAG that are presented in Sec. IV.B. We see that the algorithms that use $\alpha \in [-1, 1]$ (i.e. ST) or assume $\alpha = 1$ (i.e. AA and AAAG) outperform the algorithms that assume $\alpha = 0$ (i.e. AP and APPG) by a large margin, in terms of PESQ. In addition, in Figs. 13,14, we also observe that using $\alpha \in [-1, 1]$ is more beneficial than assuming $\alpha = 1$ for low SNR levels and a lot more beneficial than assuming $\alpha = 0$. For most SNRs, we have: $\text{AA} \geq \text{AAAG} \geq \text{AP} \geq \text{APPG}$.

Therefore, based on Figs. 13,14, utilising $\alpha \in [-1, 1]$ and $p(\alpha)$ in the signal model, and thus using that speech and noise are additive in the complex STFT domain, is beneficial.

D. Choice of tracked quantities

The next step is to compare the more complex versions of the Kalman filtering algorithm, SNT and SNPT, with ST.

We now examine the Δ PESQ of the SNT algorithm and we compare SNT with ST. We use babble noise in Fig. 15 and we observe that SNT is better than ST for $0 \leq \text{SNR} \leq 30$ dB. With NT, we track the noise log-spectrum and the correlation between the speech and noise log-spectra. The nonlinear KF update step presented in Sec. III.C and Sec. III.D estimates the correlation between the speech and noise log-spectra. With NT, we aim to approach the algorithm's maximum performance that is defined by the oracle knowledge of the actual noise power in each time-frequency cell. If we assume oracle knowledge of the actual noise power in each time-frequency cell, the median Δ PESQ at the SNR of 15 dB goes to Δ PESQ = 1.08 in Fig. 15 for babble noise.

We now concentrate on SNPT. Figure 15 is a boxplot that depicts the median and the interquartile range of the Δ PESQ scores of SNPT, SNT and ST for babble noise. Figure 15 shows that SNPT is better than SNT for $10 \leq \text{SNR} \leq 30$

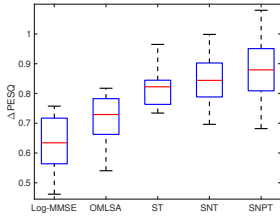


Figure 16. Boxplot of the average of the Δ PESQ scores for the noise types of car, babble, F16 and white.

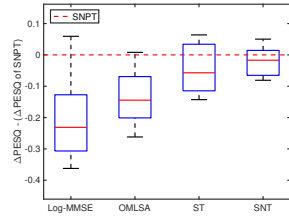


Figure 17. Boxplot of the average of the difference in Δ PESQ between competing algorithms and SNPT for car, babble, F16 and white noises.

dB. We observe that speech phase KF tracking is effective at high SNRs. Moreover, Fig. 15 shows that the SNPT, SNT and ST algorithms do not have comparable Δ PESQ variability. At SNRs from 15 dB to 30 dB, the Δ PESQ variability of SNPT is larger than the Δ PESQ variability of SNT and ST.

For F16 noise, SNPT is better than SNT for $5 \leq \text{SNR} \leq 30$ dB. Speech phase tracking is effective at high SNRs.

As in [6], to assess the robustness to noise type, we evaluate the algorithms using the four different noise types in Fig. 6 with the average SNR for each noise type chosen to give a mean PESQ score of 2.0 for the noisy speech. Combining different noise types into a single graph, Fig. 16 examines the average of the Δ PESQ scores for the noise types of car, babble, F16 and white. Based on Fig. 16 and on the Δ PESQ results in Sec. VI, the phase-aware ST block contributes the most to the final Δ PESQ of SNPT. The next most beneficial block is NT. Moreover, PT contributes further to enhancement, mainly for the SNR range of $5 < \text{SNR} \leq 30$ dB.

Figure 17 shows the average of the difference in Δ PESQ between competing algorithms and SNPT for the noise types of car, babble, F16 and white. Figure 17 uses the noise types in Fig. 6 with the average SNR for each noise type chosen to give a mean PESQ score of 2.0 for the noisy speech. According to Fig. 17, the proposed SNPT algorithm results in an improvement in Δ PESQ and thus in speech quality.

Table II

The Δ SIG, Δ BAK, Δ OVRL at different SNRs (dB) for babble noise.

	SNR = 5	SNR = 10	SNR = 15
ST			
Δ SIG	0.19	0.40	0.48
Δ BAK	0.33	0.45	0.51
Δ OVRL	0.26	0.48	0.59
SNPT			
Δ OVRL	0.23	0.49	0.61
Log-MMSE			
Δ OVRL	0.06	0.22	0.34
OMLSA			
Δ OVRL	-0.11	0.19	0.43

E. Alternative quality metrics

Speech quality metrics other than PESQ are now utilised. We use the SIG, BAK and OVRL metrics [46] [12], which are on a scale of 1 to 5 where 5 indicates excellent quality. Table II shows the SIG, BAK and OVRL of the ST, SNPT, OMLSA and Log-MMSE algorithms for babble noise.

Based on Table II, the proposed ST and SNPT algorithms improve speech quality in terms of SIG, BAK and OVRL.

VII. CONCLUSION

In this paper, we present a phase-aware single-channel enhancement algorithm that is based on tracking the time evolution of the speech log-spectrum and phase. We create a KF prediction step that models the inter-frame relations of the speech log-spectrum, the speech phase and the noise log-spectrum. In addition, we create and implement a phase-sensitive nonlinear KF update step that models the nonlinear relations between the speech log-spectrum, the speech phase and the noise log-spectrum. The nonlinear KF update step guides the model towards a good KF posterior, thus suppressing noise, using transformations of random variables and using $(s, n, \phi, \psi) \Rightarrow (u, y, \gamma, \theta)$ in Sec. III.D. We utilise both the phase difference between noise and speech, γ , and the phase difference between noisy speech and speech, δ . The time-varying KF enhances the temporal characteristics of the trajectories of the speech log-spectrum that are distorted by noise. With modulation-domain Kalman filtering, temporal constraints are imposed on the log-spectrum. Based on the evaluation in Sec. VI, the presented Kalman filtering algorithm improves speech quality; instrumental measures predict a speech quality increase over a range of SNRs for various noise types.

REFERENCES

- [1] S. So and K. K. Paliwal, "Modulation-domain Kalman filtering for single-channel speech enhancement," *Speech Communication*, vol. 53, no. 6, pp. 818-829, July 2011.
- [2] S. So, K. K. Wójcicki, and K. K. Paliwal, "Single-channel speech enhancement using Kalman filtering in the modulation domain," in *Proc. Conf. Int. Speech Communication Association, Makuhari*, Sept. 2010.
- [3] D. Liang, M. D. Hoffman and G. J. Mysore, "Speech dereverberation using a learned speech model," in *Proc. IEEE Int. Conf. Acoustics, Speech and Signal Process., Brisbane*, April 2015.
- [4] N. Boulanger-Lewandowski, G. J. Mysore and M. Hoffman, "Exploiting long-term temporal dependencies in NMF using recurrent neural networks with application to source separation," in *Proc. IEEE Int. Conf. Acoustics, Speech and Signal Process., Florence*, May 2014.
- [5] I. Andrianakis and P. R. White, "On the application of Markov Random Fields to speech enhancement," in *Proc. Int. Conf. Signal Process., pp. 198-201, Cirencester*, Dec. 2006.
- [6] Y. Wang and M. Brookes, "Speech enhancement using an MMSE spectral amplitude estimator based on a modulation domain Kalman filter with a Gamma prior," in *Proc. IEEE Int. Conf. Acoustics, Speech and Signal Process., Shanghai*, March 2016.
- [7] Y. Wang, "Speech enhancement in the modulation domain," Ph.D. dissertation, Imperial College London, 2015.
- [8] N. Mohammadiha, P. Smaragdis and A. Leijon, "Prediction based filtering and smoothing to exploit temporal dependencies in NMF," in *Proc. IEEE Int. Conf. on Acoustics, Speech and Signal Process., Vancouver*, May 2013.
- [9] J. Li, L. Deng, D. Yu, Y. Gong and A. Acero, "High-performance HMM adaption with joint compensation of additive and convolutive distortions via vector Taylor series," in *Proc. IEEE Work. Automatic Speech Recognition and Understanding*, pp. 65-70, Kyoto, Dec. 2007.

- [10] J. Li, L. Deng, D. Yu, Y. Gong and A. Acero, "A unified framework of HMM adaption with joint compensation of additive and convolutive distortions," *Computer Speech and Language*, vol. 23, no. 3, pp. 389-405, July 2009.
- [11] Y. Gong, "A method of joint compensation of additive and convolutive distortions for speaker-independent speech recognition," *IEEE Trans. on Speech Audio Process.*, vol. 13, no. 5, pp. 975-983, 2005.
- [12] P. C. Loizou, *Speech Enhancement: Theory and Practice*. Taylor & Francis, Second Edition, 2013.
- [13] J. Benesty and J. Chen, *A Conceptual Framework for Noise Reduction, Chapter 4: Single-Channel Noise Reduction in the STFT Domain with Interframe Correlation*. Springer, 2015.
- [14] N. Dionelis and M. Brookes, "Modulation-domain speech enhancement using a Kalman filter with a Bayesian update of speech and noise in the log-spectral domain," in *Proc. IEEE Int. Work. Hands-free Speech Communication and Microphone Arrays, San Francisco*, March 2017.
- [15] T. Esch and P. Vary, "Model-based speech enhancement using SNR dependent MMSE estimation," in *Proc. IEEE Int. Conf. Acoustics, Speech and Signal Process.*, pp. 4652-4655, Prague, May 2011.
- [16] T. Esch and P. Vary, "Speech enhancement using a modified Kalman filter based on complex linear prediction and supergaussian priors," in *Proc. IEEE Int. Conf. Audio and Speech Signal Process.*, pp. 4877-4880, Las Vegas, April 2008.
- [17] T. Esch and P. Vary, "Exploiting temporal correlation of speech and noise magnitudes using a modified Kalman filter for speech enhancement," in *Proc. Conf. Voice Communication (SprachKommunikation)*, pp. 1-4, Aachen, Oct. 2008.
- [18] Y. Wang and M. Brookes, "Speech enhancement using a modulation domain Kalman filter post-processor with a Gaussian mixture noise model," in *Proc. IEEE Int. Conf. Acoustics, Speech and Signal Process.*, pp. 7024-7028, Florence, May 2014.
- [19] N. Dionelis and M. Brookes, "Speech enhancement using modulation-domain Kalman filtering with active speech level normalized log-spectrum global priors," in *Proc. European Signal Process. Conf., Kos*, August 2017.
- [20] L. R. Rabiner and R. W. Schafer, *Theory and applications of digital speech Process., Chapter 9: Linear predictive analysis of speech signals*. Pearson Education, 2011.
- [21] J. Li and L. Deng and R. Haeb-Umbach and Y. Gong, *Robust automatic speech recognition, ISBN: 978-0-12-802398-3*. Elsevier, 2016.
- [22] L. Deng, J. Droppo, and A. Acero, "Enhancement of log Mel power spectra of speech using a phase-sensitive model of the acoustic environment and sequential estimation of the corrupting noise," *IEEE Trans. on Speech and Audio Process.*, vol. 12, no. 2, pp. 133-143, April 2004.
- [23] L. Deng and J. Droppo and A. Acero, "Estimating cepstrum of speech under the presence of noise using a joint prior of static and dynamic features," *IEEE Trans. on Speech and Audio Process.*, vol. 12, no. 3, pp. 218-233, May 2004.
- [24] V. Leutnant, "Bayesian estimation employing a phase-sensitive observation model for noise and reverberation robust automatic speech recognition," Ph.D. dissertation, Paderborn University, 2015.
- [25] B. Raj, R. Singh and R. Stern, "On tracking noise with linear dynamical system models," in *Proc. Conf. Int. Speech Communication Association*, pp. 965-968, Lisbon, Oct. 2004.
- [26] Matthias Wolfel, "Enhanced speech features by single-channel joint compensation of noise and reverberation," *IEEE Trans. on Audio, Speech and Language Process.*, vol. 17, no. 2, pp. 312-323, Feb. 2009.
- [27] P. Mowlae, R. Saeidi and Y. Stylianou, "Advances in phase-aware signal processing in speech communication," *Speech Communication*, vol. 81, pp. 1-29, July 2016.
- [28] V. Leutnant and R. Haeb-Umbach, "An analytic derivation of a phase-sensitive observation model for noise-robust speech recognition," in *Proc. Conf. Int. Speech Communication Association*, pp. 2395-2398, Brighton, Sept. 2009.
- [29] J. Kulmer and P. Mowlae, "Harmonic phase estimation in single-channel speech enhancement using von Mises distribution and prior SNR," in *Proc. IEEE Int. Conf. Audio and Speech Signal Process., Brisbane*, April 2015.
- [30] G. Kurz, I. Gilitschenski and U. D. Hanebeck, "Recursive Bayesian filtering in circular state spaces," *IEEE A&E Systems Magazine*, vol. 31, no. 3, pp. 70-87, DOI: No. 10.1109/MAES.2016.150083, March 2016.
- [31] M. Krawczyk and T. Gerkmann, "STFT phase reconstruction in voiced speech for an improved single-channel speech enhancement," *IEEE/ACM Trans. on Audio, Speech, and Language Process.*, vol. 22, no. 12, pp. 1931-1940, Dec. 2014.
- [32] T. Esch, "Model-based speech enhancement exploiting temporal and spectral dependencies," Ph.D. dissertation, Aachen University, 2012.
- [33] N. Dionelis and M. Brookes, "Active speech level estimation in noisy signals with quadrature noise suppression," in *Proc. European Signal Process. Conf., Budapest*, Aug. 2016.
- [34] Y. Ephraim and D. Malah, "Speech enhancement using a minimum mean-square error log-spectral amplitude estimator," *IEEE Trans. on Acoustics, Speech and Signal Process.*, vol. 33, no. 2, pp. 443-445, April 1985.
- [35] C.-F. C. R. Chen and H. C. So, "Model-based speech enhancement with improved spectral envelope estimation via dynamics tracking," *IEEE Trans. on Audio, Speech, and Language Process.*, vol. 20, no. 4, pp. 1324-1336, May 2012.
- [36] J. Garofolo, L. Lamel, W. Fisher et al., "TIMIT acoustic-phonetic continuous speech corpus," *Corpus LDC93S1, Linguistic Data Consortium, Philadelphia*, 1993.
- [37] H. Steeneken and F. Geurtsen, "Description of the RSG-10 noise database," *TNO Institute for perception*, 1988.
- [38] M. Brookes, "VOICEBOX: A speech processing toolbox for MATLAB," 1997-2017.
- [39] T. Gerkmann and R. C. Hendriks, "Unbiased MMSE-based noise power estimation with low complexity and low tracking delay," *IEEE Trans. on Audio, Speech, and Language Process.*, vol. 20, no. 4, pp. 1383-1393, 2012.
- [40] S. J. Julier and J. K. Uhlmann, "Unscented filtering and nonlinear estimation," *Proceedings of the IEEE*, vol. 92, no. 3, pp. 401-422, March 2004.
- [41] C. S. J. Doire, M. Brookes, P. A. Naylor et al., "Single-channel online enhancement of speech corrupted by reverberation and noise," *IEEE/ACM Trans. on Audio, Speech and Language Process.*, vol. 25, no. 3, pp. 572-587, March 2017.
- [42] N. Dionelis and M. Brookes, "Phase-aware single-channel speech enhancement with modulation-domain Kalman filtering: Listening examples and proof of concept," 2017, [Online] <https://www.dropbox.com/sh/loc9e0xptydde0m/AAApES4cXFCBF3K1MjDFkz6ba?dl=0>.
- [43] I. Cohen and B. Berdugo, "Speech enhancement for non-stationary noise environments," *Signal Processing*, vol. 81, no. 11, pp. 2403-2418, 2001.
- [44] Cohen, I. and Berdugo, B., "Noise estimation by minima controlled recursive averaging for robust speech enhancement," *IEEE Signal Processing Letters*, vol. 9, pp. 12-15, 2002.
- [45] ITU-T, "Perceptual evaluation of speech quality (PESQ), an objective method for end-to-end speech quality assessment of narrowband telephone networks and speech codecs," ITU-T Rec P.862, Feb. 2001.
- [46] Y. Hu and P. Loizou, "Evaluation of objective measures for speech enhancement," in *Proc. Conf. Int. Speech Communication Association, Pittsburgh*, Sept. 2006.